

Off-Line Parameter Identification of Interior Permanent Magnet Motor by Searching Minimum Point of Current Norm Characteristics

Xiang Ji

Department of Environment and Energy Systems,
Graduate School of Science and Technology,
Shizuoka University
Hamamatsu, Shizuoka 432-8561, Japan
f5345014@ipc.shizuoka.ac.jp

Toshihiko Noguchi

Department of Electrical and Electronics Engineering,
Graduate School of Engineering,
Shizuoka University
Hamamatsu, Shizuoka 432-8561, Japan
tnogut@ipc.shizuoka.ac.jp

Abstract—This paper describes a novel parameter identification technique of an interior permanent magnet (IPM) motor. The controller of the IPM motor requires its parameters in the decoupled current control loops. Off-line parameter tuning is indispensable to achieve initial setup and starting up of the motor control. The proposed technique can tune the every motor parameter by changing the current controller structure and by seeking the minimum point of the current norm on the basis of a hill-climbing algorithm. The paper presents some simulation results of the identification of the d-axis inductance, q-axis inductance, magnetic flux linkage, and winding resistance, followed by the theoretical analysis. In the end of the paper, the experimental test results of the q-axis inductance and winding resistance identification are demonstrated to confirm the feasibility of the proposed technique.

Keywords— *identification; parameter; IPMSM; hill-climbing; current norm; minimum point; current controller.*

I. INTRODUCTION

In recent years, interior permanent magnet (IPM) motors are widely used in a variety of industry, home appliance, and automotive applications, owing to its high-efficiency and high-power-density features. The IPM motor is usually controlled with a field-orientation technique (vector control), and requires a current controller on the synchronous rotating reference frame (dq-reference-frame) for the instantaneous torque and magnetic flux control. The current control on the dq-reference-frame mainly consists of the coordinate transformation, the PI regulation, and the decoupling compensation, which is based on the mathematical model of the motor. Therefore, it is indispensable not only to detect the magnetic-pole-position and the motor currents but also to know the motor parameters accurately. Identification of the motor parameters is important to control the motor properly in starting up of the control as well as the running operation, and the off-line parameter identification is particularly required for the initial controller setup and starting up. There are four parameters to be off-line identified in the motor model, i.e., the d-axis inductance L_d , the q-axis inductance L_q , the magnetic flux linkage ψ , and the winding resistance R . Each

of the motor parameters must be identified individually in as a simple manner as possible.

This paper proposes a novel technique to achieve the off-line identification of the IPM motor parameters, which requires only the motor current norm information. The proposed technique has several steps to complete the identification of the all parameters, where the current controller structure is changed every time the identification step proceeds, and the minimum operation point of the current norm is sought by tuning the specific motor parameter until the parameter mismatch is cancelled out. The search for the current norm minimum point is achieved by an ordinary hill-climbing algorithm with respect to the parameter mismatch. In the following sections, some theoretical analyses are developed, followed by the simulation results, and experimental test results are also presented to show the feasibility of the proposed technique.

II. OFF-LINE PARAMETER IDENTIFICATION USING CURRENT NORM CHARACTERISTICS

In the standard control system of the IPM motor, the field-oriented control (the vector control) technique is often used to control the instantaneous torque and the magnetic flux. The field-orientation is achieved by controlling the two-axis armature current components, i.e., the d-axis current and the q-axis current on the synchronously rotating dq-reference-frame. Figure 1 shows the whole system block diagram including the decoupling current controller and the IPM motor. In the figure, the three-to-two-phase coordinate transformation and the rotational coordinate transformation are omitted for convenience because the magnetic-pole-position is accurately acquired by the mechanical position sensor such as a rotary encoder or a resolver. As can be seen in the block diagram, several motor parameters are required to compose the two-axis current control loops and to control the two-axis currents independently. The motor parameters can be simply calculated by using the voltage and current information on the basis of the inverse motor model. However, detecting the real voltage is not pragmatic because no voltage sensors are

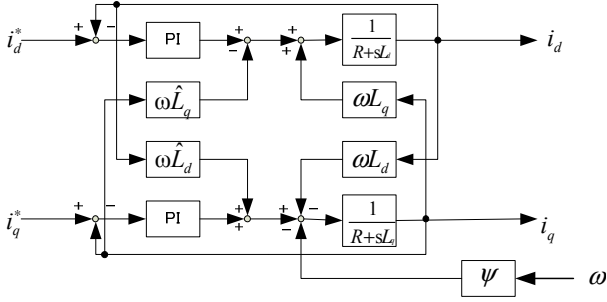


Fig. 1. Decoupling current control system of IPM motor.

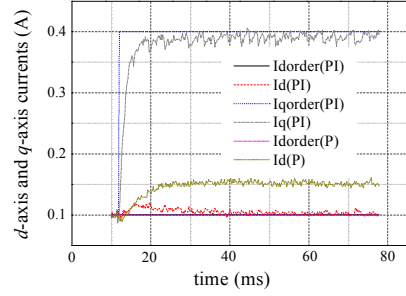


Fig. 4. Current step responses of P and PI regulators.

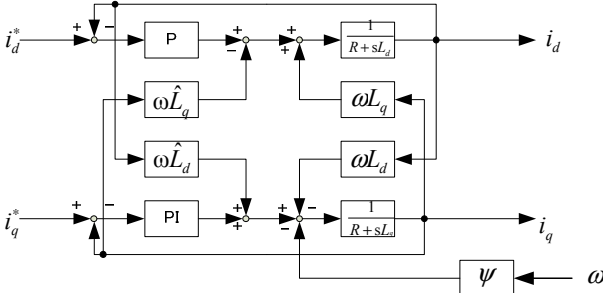


Fig. 2. Structure of current control loops on L_q identification.

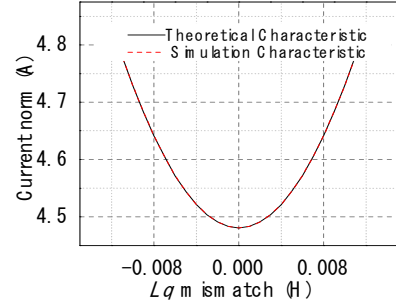


Fig. 5. Simulation result of motor current norm characteristic with respect to L_q mismatch.

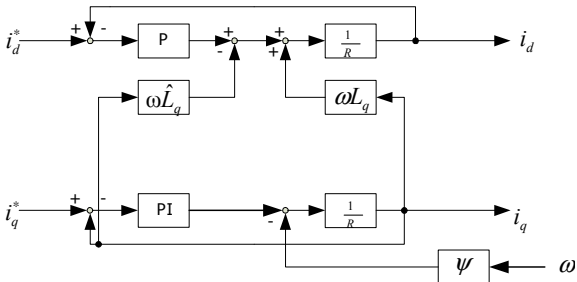


Fig. 3. Simplified current control loops on L_q identification.

installed in the standard controller. Even though the voltage commands generated by the current regulators are used instead of the real voltages, there must be errors in the voltage commands because of the dead time and the voltage drop of the power transistors in the inverter. On the other hand, the accurate current detection is inherently available in the controller by employing some Hall-effect current transducers. It is the simplest and pragmatic way, therefore, to utilize only the current information without any complicated mathematical calculation in the motor parameter identification. In addition, it is necessary to avoid the undesirable mutual interferences among the parameters in each parameter identification process.

In order to achieve this goal, the proposed technique introduces modifications of the current control loop structure, and focuses on the motor current norm characteristics with respect to the parameter mismatches.

A. Identification of L_q

In the case of the L_q identification, the structure of the current control loops is changed as shown in Fig. 2, where the d-axis PI regulator is replaced with a low-gain P regulator to let the current norm have a large variation. On the contrary,

the q-axis current regulator remains the PI form to suppress the interferences from the d-axis and the back electromotive force (e.m.f.). No matter how much parameter mismatch exists between the real d-axis inductance L_d and the set value \hat{L}_d in the controller, the steady state error of the q-axis current is perfectly eliminated because the PI regulator is employed in the q-axis current loop, i.e., $i_q^* = i_q$ is guaranteed in the steady state. Therefore, the modified current controller in Fig. 2 can be simplified as shown in Fig. 3 in the steady state. The q-axis PI regulator has the following transfer function:

$$G_{PIq}(s) = K_{Pq} \left(1 + \frac{1}{s \tau_{Iq}} \right). \quad (1)$$

In the above transfer function, the P gain K_{Pq} and the integral time constant τ_{Iq} are designed as follows:

$$K_{PI} = \omega_c L_q \quad \text{and} \quad \tau_q = \frac{L_q}{R}, \quad (2)$$

TABLE I PARAMETERS USED IN SIMULATION.

Symbol	Description	Value
R	Winding resistance	0.48 Ω
P	Rated output power	1.5 kW
ζ	Damping coefficient	0.0002 Ns/r
p	Number of poles	4
ω	Rotation speed	50 r/s
ψ	Magnetic flux linkage	0.0674 Wb
L_q	q-axis inductance	12.0 mH
L_d	d-axis inductance	7.3 mH
K_{Pd}	P Gain of d-axis regulator	1.0 V/A

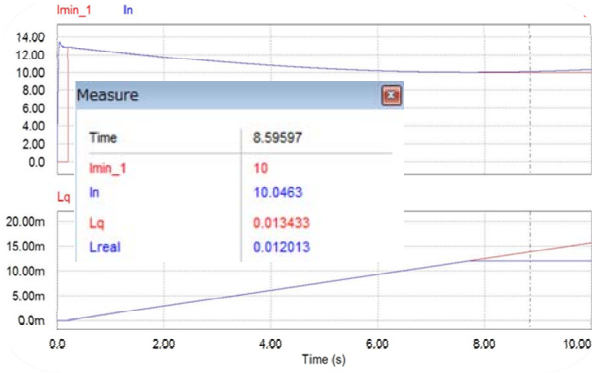


Fig. 6. Simulation result of proposed L_q identification technique.

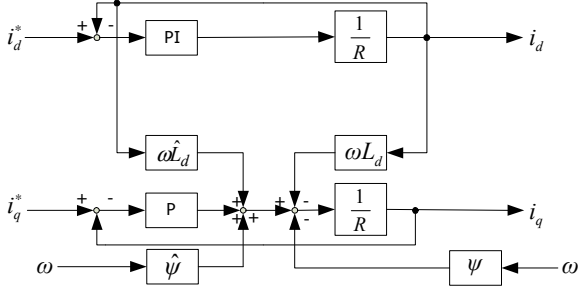


Fig. 7. Structure of current control loops on ψ and L_d identification.

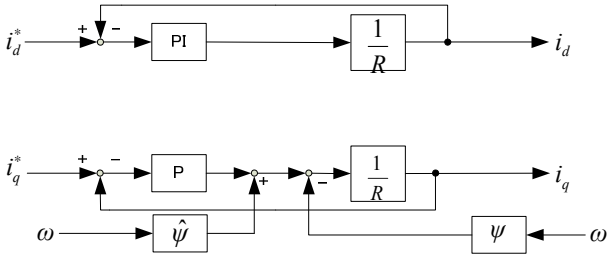


Fig. 8. Simplified current control loops on ψ and L_d identification when $i_d^* = 0$.

where ω_c is a designed crossover frequency of the q-axis current control loop. Figure 4 shows an example of the current step responses of the P-regulator-based d-axis and the PI-regulator-based q-axis current control loops. As can be seen in the figure, the d-axis current control loop has a large steady state error after the q-axis current command is given to the system.

From the simplified current controller shown in Fig. 3, the following relationship is mathematically derived:

$$i_q = i_q^* \quad (3)$$

$$i_d = \frac{i_q^* \omega_c (\hat{L}_q - L_q)}{K_{Pd} + R}, \text{ and} \quad (4)$$

$$i_n = \sqrt{i_d^2 + i_q^2}. \quad (5)$$

In the above equations, i_n is the motor current norm. It is found that i_n is a parabolic function of the L_q mismatch and that it takes the minimum value when the L_q mismatch is completely canceled out. It should be also noted that i_n always

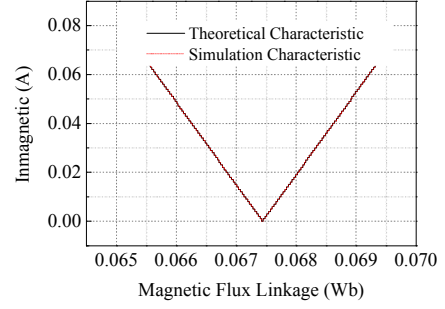


Fig. 9. Simulation result of motor current norm characteristic with respect to ψ mismatch.

TABLE II PARAMETERS USED IN SIMULATION.

Symbol	Description	Value
ψ	Magnetic flux linkage	0.0674 Wb
$\hat{\psi}$	Initial set value of magnetic flux linkage	0 Wb
L_q	q-axis inductance	12.0 mH
L_d	d-axis inductance	7.3 mH
\hat{L}_d	Initial set value of d-axis inductance	0 mH
K_{Pd}	P Gain of q-axis regulator	1.0 V/A

becomes minimum when $\hat{L}_q = L_q$ regardless of any other variable and parameter values i_q^* , ω_c , K_{Pd} , and R . Figure 5 shows a simulation result of the current norm characteristic with respect to the L_q mismatch. The simulation condition is listed in TABLE I. This current norm characteristic is obtained by gradually changing the set value of L_q in the controller. As illustrated in the figure, the current norm has a parabolic function characteristic whose minimum point can be observed when the L_q mismatch becomes zero. In other words, the real value of the q-axis inductance can be estimated by searching the minimum point of the current norm characteristic. This search operation is carried out by means of a hill-climbing algorithm.

Figure 6 shows another simulation result of the L_q identification with the interferences from the d-axis and the back e.m.f. It is observed from the result that the current norm reaches the minimum value when the set value of the q-axis inductance also reach the real value of the motor. The result proves robustness of the proposed identification technique against the other parameter mismatches of L_d and ψ in the steady state.

B. Identification of ψ

In a similar manner, ψ and L_d can be identified with the same approach. However, some minor modification is required to identify these parameters separately. After L_q is identified as described in the previous section, the current loop structure is changed to that shown in Fig. 7. Figure 7 shows the structure of the current control loops changed for the ψ and L_d identifications, where the d-axis employs the PI regulator but the q-axis current regulator is replaced with a low-gain P regulator. Therefore, the steady state error in the d-axis current control loop is perfectly eliminated, but the q-axis current involves some amount of steady state error due to the back e.m.f. and the L_d mismatch. In order to carry out the

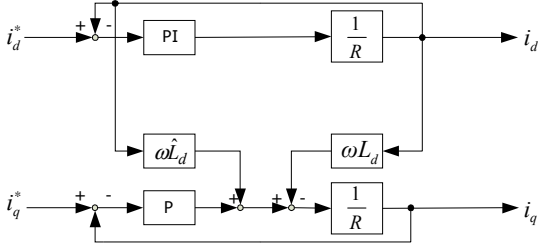


Fig. 10. Simplified current control loops on L_d identification.

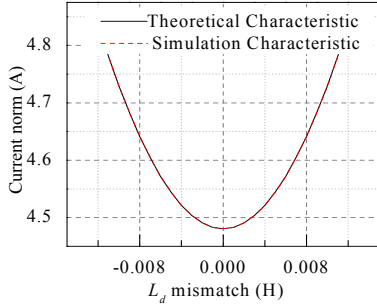


Fig. 11. Simulation result of motor current norm characteristic with respect to L_d mismatch.

separate identification of the two parameters, the identification process is divided into the following two steps.

In the first identification step of ψ , the d-axis current command $i_d^* = 0$ is given to the controller. Since the d-axis current control loop employs the PI regulator, $i_d = 0$ is achieved with no steady state error. In addition, a cross decoupling term through ωL_d and $\omega \hat{L}_d$ from the d-axis to the q-axis can be ignored because $i_d = 0$ is guaranteed. In this case, only the parameter mismatch of ψ affects the steady state error of the q-axis current. Taking the above discussion into account, the current controller structure can be simplified as shown in Fig. 8, where the back e.m.f. compensation block is virtually added to the q-axis current control loop in the controller for the purpose of the ψ identification.

Mathematical expressions of i_d and i_q can be derived from Fig. 8 as presented by (6) and (7):

$$i_d = i_d^* = 0, \text{ and} \quad (6)$$

$$i_q = \frac{\omega_c (\hat{\psi} - \psi)}{K_{Pq} + R} + \frac{i_q^* K_{Pq}}{K_{Pq} + R}. \quad (7)$$

The second term of (7) affects the identification of ψ , so this part must be eliminated from the calculation without using the winding resistance of the motor. This can be done by using the d-axis current control loop as a simulator of the second term in (7). As mentioned previously, d-axis current control loop no longer has any interference from the q-axis because L_q is already identified and $\hat{L}_q = L_q$. Therefore, if the d-axis current regulator is changed to a P regulator whose gain is

equal to K_{Pq} and the d-axis current command is changed to the value equal to i_q^* , the resultant d-axis current comes to have the same value as the second term of (7). This implies that the second term of (7) can be found with no knowledge of the winding resistance. By memorizing the simulated second term value and by subtracting the memorized value from (7), the most important part can be extracted from (7) as follows:

$$i_q' = \frac{\omega_c (\hat{\psi} - \psi)}{K_{Pq} + R}. \quad (8)$$

By using (8), the motor current norm is expressed as

$$i_n = \sqrt{i_d^2 + i_q'^2} = \frac{\omega_c (\hat{\psi} - \psi)}{K_{Pq} + R}. \quad (9)$$

Figure 9 shows a simulation result of the current norm characteristic when the ψ mismatch is varied by gradually changing the set value in the controller, and the simulation conditions are listed in TABLE II. As expressed by (9), the current norm characteristic is linear as a function of the ψ mismatch. The current norm i_n has the minimum value when the ψ mismatch becomes zero, where the minimum point of i_n can be sought by means of the hill-climbing algorithm, also.

C. Identification of L_d

After identification of L_q and ψ , the identification of L_d is carried out in the similar manner as described in the previous sections. This identification is still based on the system configuration shown in Fig. 7. The only difference between the case of the ψ identification is the operating condition of the system, i.e., $i_q^* = 0$ and $i_d^* \neq 0$ are given to the system. In the case, the current controller is simplified as shown in Fig. 10, and its mathematical expressions in terms of the d-axis and q-axis currents can be derived from the block diagram as follows:

$$i_q = \frac{i_d^* K_{Pd} \omega_c (\hat{L}_d - L_d)}{(K_{Pq} + R)(K_{Pd} + R)}, \quad (10)$$

$$i_d = \frac{i_d^* K_{Pd}}{K_{Pd} + R}, \text{ and} \quad (11)$$

$$i_n = \sqrt{i_d^2 + i_q^2}. \quad (12)$$

Figure 11 shows a simulation result of the current norm i_n with respect to the L_d mismatch. As can be seen in the figure, the current norm curve has a parabolic characteristic as a function of the L_d mismatch. It should be noted that i_n becomes minimum only at the point of $\hat{L}_d = L_d$ as the L_d mismatch is varied by changing the set value in the controller; hence, it is possible to identify L_d by adopting the similar hill-climbing algorithm as described previously. In addition, the minimum point of i_n can be observed only when $\hat{L}_d = L_d$, no matter how much the winding resistance R varies. This means that the proposed method is basically robust to the temperature variation of the windings and the motor cable length.

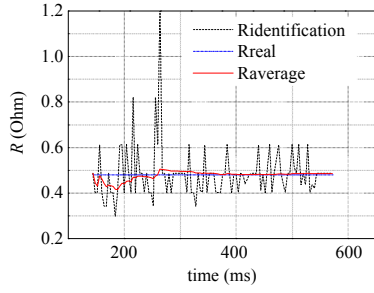


Fig. 12. Experimental result of R identification.



Fig. 13. Experimental setup.

TABLE III OPERATION PARAMETERS OF EXPERIMENTAL TEST.

Symbol	Description	Value
R	Winding resistance	0.48Ω
P	Rated output power	1.5 kW
ζ	Damping coefficient	0.0002 Ns/r
p	Number of poles	6
ω	Rotation speed	5.33 r/s
ψ	Magnetic flux linkage	0.0674 Wb
$\hat{\psi}$	Initial set value of Magnetic flux linkage	0 Wb
L_q	q-axis inductance	24.5 mH
\hat{L}_q	Range of q-axis inductance	16.0~36.0 mH
L_d	d-axis inductance	13.0 mH
\hat{L}_d	Initial set value of d-axis inductance	10.0 mH
K_p	Gain of P regulator	1.0 V/A
K_{pl}	Gain of PI regulator	0.131 V/A
τ_l	Time constant of PI regulator	0.051 s
i_q^*	q-axis current command	1.6 A

D. Identification of R

As described in the above discussion, the proposed identification technique of the IPM motor parameters does not require any information of the winding resistance R , and is basically robust to the variation of R ; thus, it is not necessary to identify R inherently. The R identification, however, can be optionally realized by using the identification algorithms described so far.

From (11), R is simply calculated by the following expression:

$$R = \frac{K_{pd} (i_d^* - i_d)}{i_d} \quad (13)$$

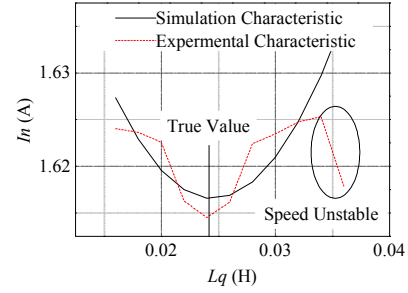


Fig. 14. Motor current norm characteristics calculated by simulation and traced by proposed identification technique with respect to L_q mismatch.

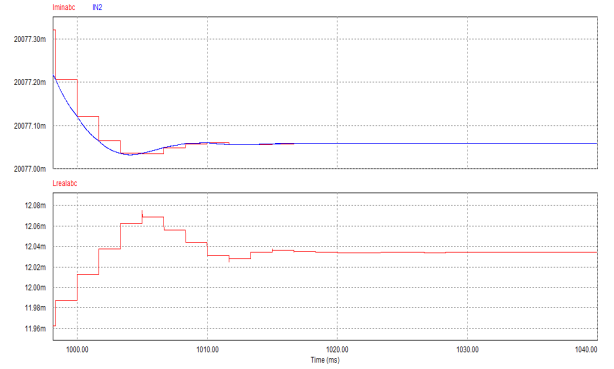


Fig. 15. Simulation result of L_q identification by using hill-climbing algorithm.

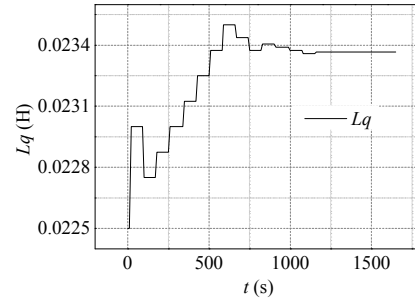


Fig. 16. Experimental result of L_q identification by using hill-climbing algorithm.

Figure 12 shows an example of the experimental test result of the R identification. The black line is the winding resistance value calculated by (13), and the red line is its average value. As can be seen in the figure, the average value of R converges to the true value that has been measured by the parameter measurement test. The identified average value is 0.485Ω , while the true value is 0.48Ω , where the identification error is approximately 1%.

III. EXPERIMENTAL SETUP AND TEST RESULTS

Experimental tests were conducted with the experimental setup shown in Fig. 13, where the two same IPM motors were mechanically connected through the torque meter. One motor is controlled by the current controller as shown in Fig. 1, and the other is used merely as a generator with load resistors. The operation parameters of the experimental setup are listed in TABLE III, whose most parameters are the same as those used in the simulations. Attention must be paid to the initial

parameter values set in the controller, i.e., ψ and L_d intentionally have the initial errors. These errors make it possible to verify the robustness of the proposed identification technique. Prior to the experimental tests of the proposed technique, the relationship between the motor current norm and the L_q mismatch was confirmed, where the set value in the controller \hat{L}_q had the tuning range from 16.0 to 36.0 mH as indicated in TABLE III.

Figure 14 shows the motor current norm characteristics obtained by the simulation and the experimental test, where the black and the red lines are the simulation and the experimental results, respectively. As can be seen in the graph, the two curves have the minimum points at the same values of L_q . However, the experimental test was broken off in the range of the high L_q region, and the parabolic characteristic was lost due to the unstable rotation of the test motor.

As the parabolic characteristic was confirmed in the above preliminary test, the simulation adopting the hill-climbing algorithm was conducted to check the dynamic behavior of the L_q identification. Figure 15 shows the simulation result. It is found that the set value in the controller converges to the true value within the identification error of 0.3 %.

Figure 16 shows the experimental result of the proposed technique. The dynamic convergence behavior of the set value of L_q has a slight overshoot with a damping, and the final converged value is 23.4 mH. The true value of L_q is 24.5mH, so the identification error is 4.5 % in the test. From this result, the proposed technique is capable to identify L_q stably within the error of approximately ± 5 %. It is considered that the identification error is caused by the following possible reasons:

- 1) ripples of the motor current norm, and
- 2) undesirable fluctuation of the low-rotation-speed, which has an impact to the current norm.

To overcome these problems, the following countermeasures can be effective solutions:

- 1) reduction of ripple effects using averaging scheme of the motor current norm, and
- 2) testing in higher speed region to reduce the fluctuated speed effect or adding the speed control loop to the proposed identification system to make the speed control more stable.

IV. CONCLUSION

The off-line identification technique of the IPM motor parameters has been proposed in this paper. The most unique feature of the technique is capability to identify the parameters by using only the motor current norm information and robustness to the winding resistance variation. The identification proceeds step by step with changing the structure of the current controller and with seeking the minimum point of the current norm on the basis of the well-known hill-climbing algorithm. The identification of the

motor parameters can be achieved because the minimum point of the current norm is found only when the parameter mismatch is cancelled out between the controller and the real motor. The proposed identification technique is also theoretically proven by the mathematical model of the IPM motor drive.

Several simulations have been conducted to check the motor current norm characteristics and the identification process of the motor parameters. In addition, the experimental test of the L_q identification has been conducted to confirm the performance of the proposed technique as an example. The resultant error of the L_q identification is approximately 4.5 %. In the end of the paper, the reasons of this identification error has been discussed. Furthermore, the winding resistance identification technique has been also discussed, which was an optional function of the proposed identification technique because the technique basically requires no knowledge of the resistance.

Identification of ψ and L_d will be also examined through the experimental tests in the future work to confirm total feasibility of the proposed technique. In addition, improvement of the identification accuracy will be considered on the basis of the discussion suggested in this work.

REFERENCES

- [1] Masaki Ohara and T. Noguchi, "Sensorless Control of Permanent Motor Based on Model Reference Adaptive System," IEEJ Annu. Conf. Proc., no. 4, #107, pp. 183-184, 2010.
- [2] Toshihiko Noguchi, Shigenori Togashi, and Ryo Nakamoto, "Short-Current Pulse-Based Maximum-Power-Point Tracking Method for Multiple Photovoltaic-and-Converter Module System," IEEE Trans. on Ind. Elec., vol. 49, no. 1, pp. 217-222, 2002.
- [3] P. Pillay and R. Krishnan, "Modeling Analysis and Simulation of High Performance Vector Controlled Permanent Magnet Synchronous Motor Drive," IEEE Ind. Appl. Soc. Annu. Meet. Conf. Proc., Atlanta, 1987.
- [4] M. Lajoie-Mazenc, C. Villanueva, and I. Hector, "Study and Implementation of a Hysteresis Controlled Inverter on a Permanent Magnet Synchronous Machine," IEEE Trans. Ind. Appl., vol. 1A-21, no. 2, pp. 408-413, 1985.
- [5] A. Mujanovic, P. Crnosija, and Z. Ban, "Determination of Transient Error and Signal Adaptation Algorithm Coefficients in MRAS," Proc. of IEEE Int. Symp. on Ind. Elec., pp. 631-634, Maribor, 1999.
- [6] Y. Liang and Yongdong Li, "Sensorless Control of PM Synchronous Motors Based on MRAS Method and Initial Position Estimation," Proc. of ICEMS 2003, vol. 1, pp. 96-99, 2003.
- [7] H. W. Kim, N. V. Nho, and M. J. Youn, "Current Control of PM Synchronous Motor in Overmodulation Range," Proc. of IECON 2004, pp. 896-901, 2004.
- [8] J. K. Seok, K. T. Kim, and D. C. Lee, "Automatic Mode Switching of P/PI Speed Control for Industry Servo Drives Using Online Spectrum Analysis of Torque Command," IEEE Trans. on Ind. Elec., vol. 54, pp. 2642-2647, 2007.
- [9] J. K. Seok, "Frequency-Spectrum-Based Antiwindup Compensator for PI Controlled Systems," IEEE Trans. on Ind. Elec., vol. 53, pp. 1781-1790, 2006.
- [10] K. Paponpen and M. Konghirum, "An Improved Sliding Mode Observer for Speed Sensorless Vector Control Drive System," IEEE Power Elec. and Motion Cont. 5th Int. Conf., vol. 2, 2006.